American Journal of Energy Engineering
2015; 3(4-1): 42-51
Published online February 14, 2015 (http://www.sciencepublishinggroup.com/j/ajee)
doi: 10.11648/j.ajee.s.2015030401.13
ISSN: 2329-1648 (Print); ISSN: 2329-163X (Online)

Investigation of Unsteady Mixed Convection Flow near the Stagnation Point of a Heated Vertical Plate embedded in a Nanofluid-Saturated Porous Medium by Self-Similar Technique

A. A. Abdullah[1], F. S. Ibrahim[2], A. F. Abdel Gawad[3], A. Batyyb[3]

[1]Department of Mathematical Sciences, Umm Al-Qura University, Makkah, Saudi Arabia
[2]Department of Mathematics, University College, Umm Al-Qura University, Makkah, Saudi Arabia
[3]Mech. Eng. Dept., College of Engineering and Islamic Architecture, Umm Al-Qura University, Makkah, Saudi Arabia

Email address:
batyyb@hotmail.com (A. Batyyb)

To cite this article:
A. A. Abdullah, F. S. Ibrahim, A. F. Abdel Gawad, A. Batyyb. Investigation of Unsteady Mixed Convection Flow near the Stagnation Point of a Heated Vertical Plate embedded in a Nanofluid-Saturated Porous Medium by Self-Similar Technique. *American Journal of Energy Engineering*. Special Issue: Computational Simulation of Fire and Evacuation. Vol. 3, No. 4-1, 2015, pp. 42-51.
doi: 10.11648/j.ajee.s.2015030401.13

Abstract: This paper aims to study the problem of unsteady mixed convection in a stagnation flow on a heated vertical surface embedded in a nanofluid-saturated porous medium. The employed mathematical model for the nanofluid takes into account the effects of Brownian motion and thermophoresis. The presence of a solid matrix, which exerts first and second resistance parameters, is considered in this study. The self-similar solutions for the system of equations governing the problem are obtained. The resulting system of ordinary differential equations that govern the flow is solved numerically using fourth-fifth order Runge-Kutta with shooting method. Numerical results for the dimensionless velocity, temperature and nanoparticle volume fraction as well as skin friction, Nusselt number and Sherwood number are produced for different values of the influence parameters.

Keywords: Unsteady Mixed Convection, Self-Similar Solution, Nanofluids, Stagnation, Porous Media

1. Introduction

The study of mixed convection flow has applications in several industrial and technical processes such as nuclear reactors cooled during emergency shutdown, solar central-receivers exposed to winds, electronic devices cooling by fans, heat exchanges placed in a low-velocity environment, etc. The mixed convection flows become important when the buoyancy forces, due to the temperature difference between the wall and the free stream, become large. The mixed convection flow in the stagnation flow region of a vertical plate has been investigated by Ramachandra et al. [1].

When there is an impulsive change in the velocity field, the inviscid flow develops instantaneously, but the flow in the viscous layer near the wall develops slowly which becomes fully-developed steady flow after sometime. For a small period of time, the flow is dominated by the viscous forces and the unsteady acceleration, but for a large period of time, it is dominated by the viscous forces, the pressure gradient and the convective acceleration. Scshadri et al. [2] studied the unsteady mixed convection flow in the stagnation region of a heated vertical plate due to impulsive motion. The boundary-layer flow development of a viscous fluid on a semi-infinite flat plate due to impulsive motion of the free stream was investigated by Hall [3], Dennis [4] and Watkins [5]. The corresponding problem over a wedge was studied by Smith [6], Nanbu [7], and Williams and Rhyne [8].

Kumari [9] examined the temporal development of momentum and thermal boundary layers on an impulsively-started wedge with a magnetic field and has obtained the solution numerically starting from the initial steady state to the final steady state. The flow development of the laminar boundary on an impulsively-started translating and spinning rotational symmetric body was considered by Ece [10]. Qzturk and Ece [11] studied the unsteady forced convection heat transfer from a translating and spinning body. Brown and Riley [12] presented an analysis that covered three

distinct phases in the temporal development of the free convection flow past a suddenly heated semi-infinite vertical plate. The unsteadiness in the flow field arises due to the step change in wall temperature. Ingham [13] has considered essentially the same problem as that of Brown and Riley [12], but instead of taking the step change in wall temperature, the wall temperature T_∞ is suddenly raised to $T_w = T_\infty + Ax^m$, where A is a positive constant, m is a constant and x is the distance measured from the leading edge of the plate.

The mixed convection flow at a two-dimensional stagnation point was investigated by Amin and Riley [14]. The forced flow is a stagnation point flow and the free convection part is due to a pressure gradient that is induced by temperature variations along the boundary. Hassanien, et al. [15] analyzed the problem of unsteady free convection flow in the stagnation-point region of a rotating sphere embedded in a porous medium. The unsteady flow and heat transfer of a viscous fluid in the stagnation region of a three-dimensional body embedded in a porous medium was investigated by Hassanien, et al. [16]. Hassanien and Al-Arab [17] studied the problem of thermal radiation and variable viscosity effects on unsteady mixed convection flow in the stagnation region on a vertical surface embedded in a porous medium with surface heat flux

The research topic of nanofluids has received considerable interest worldwide. Inherently low thermal conductivity is a primary limitation in developing energy-efficient heat transfer fluids that are required for ultrahigh-performance cooling. A very small amount of guest nanoparticles, when dispersed uniformly and suspended stably in host fluids, can provide dramatic improvements in the thermal properties of the host fluids. According to Yacob et al. [18], nanofluids are produced by dispersing the nanometer-scale solid particles into base liquids with low thermal conductivity such as water and ethylene glycol. Nanoparticles are usually made of metal, metal oxide, carbide, nitride and even immiscible nano-scale liquid droplets. Congedo et al. [19] compared different models of nanofluid (regarded as a single phase) to investigate the density, specific heat, viscosity and thermal conductivity and discussed the water–Al2O3 nanofluid in details by using CFD. Hamad et al. [20] introduced a one-parameter group to represent similarity reductions for the problem of magnetic field effects on free-convective nanofluid flow past a semi-infinite vertical flat plate following a nanofluid model proposed by Buongiorno [21]. Hamad [22] obtained the analytical solutions for convective flow and heat transfer of a viscous incompressible nanofluid past a semi-infinite vertical stretching sheet in the presence of magnetic field. Khan and Pop [23] obtained similarity solutions depending on Prandtl, Lewis, Brownian motion and thermophoresis numbers on the steady boundary-layer flow, heat and mass over a stretching surface in its plane. Further, Abu-Nada and Chamkha [24] presented the natural convection heat transfer characteristics in a differentially-heated enclosure filled with a CuO–EG–water nanofluid for different variable thermal conductivity and variable viscosity models. For more information, see also Das et al. [25], and Kakaç and Pramuanjaroenkij [26]. Muthtamilselvan et al. [27] claimed that it is difficult to have a precise idea on how nanoparticles enhance the heat transfer characteristics of nanofluids.

In this study, our main objective is to analyze mixed convection in stagnation flow on a heated vertical surface embedded in a nanofluid-saturated porous medium. The effect of the presence of an isotropic solid matrix due to impulsive motion is considered. Moreover, we examine the combined effect of Brownian motion, thermophoresis parameters and nanoparticle fraction on boundary-layer flow and heat transfer and due to nanofluid. The governing boundary layer equations are transformed to a two-point boundary-value problem using similarity variables. These are numerically solved using fourth-fifth order Runge–Kutta method with shooting technique. The effects of governing parameters on fluid velocity, temperature and particle concentration are discussed and shown graphically and in tables as well.

2. Mathematical Analysis

Let us consider a semi-infinite vertical plate embedded in a saturated porous medium with temperature T_w and concentration ϕ_w. The ambient temperature and concentration, respectively are T_∞ and. ϕ_∞. At $t = 0.0$ the ambient fluid is impulsively moved with a velocity U_e and at the same time the surface temperature is suddenly raised. The flow field is over a heated vertical surface where the upper half of the field is assisted by the buoyancy force. However, the buoyancy force opposes the lower part. The surface of the plate is assumed to have arbitrary temperature and concentration. The physical flow model and coordinate system is shown in Fig. 1.

Under above assumptions along with Boussinesq and boundary layer approximations, the governing equations of the conservation of mass, momentum, energy and nanoparticles volume fraction can be expressed as:

$$\frac{\partial u}{\partial x} + \frac{\partial v}{\partial y} = 0 \ , \tag{1}$$

$$\frac{\partial u}{\partial t} + u\frac{\partial u}{\partial x} + v\frac{\partial u}{\partial y} = \frac{\partial U_e}{\partial t} + U_e\frac{\partial U_e}{\partial x} + \nu\frac{\partial^2 u}{\partial y^2} + \frac{\nu}{K}(U_e - u) + \frac{\Gamma}{K^{1/2}}(U_e^2 - u^2) + [(1-\phi_\infty)\beta(T - T_\infty) - (\rho_p - \rho_f)(\phi - \phi_\infty)/\rho_f]g \tag{2}$$

$$\frac{\partial T}{\partial t} + u\frac{\partial T}{\partial x} + v\frac{\partial T}{\partial y} = \alpha\frac{\partial^2 T}{\partial y^2} + \tau\left[D_B\frac{\partial T}{\partial y}\frac{\partial \phi}{\partial y} + \frac{D_T}{T_\infty}\left(\frac{\partial T}{\partial y}\right)^2\right], \tag{3}$$

$$\frac{\partial \phi}{\partial t} + (u\frac{\partial \varphi}{\partial x} + v\frac{\partial \phi}{\partial y}) = D_B\frac{\partial^2 \phi}{\partial y^2} + \frac{D_T}{T_\infty}\left(\frac{\partial^2 T}{\partial y^2}\right), \tag{4}$$

Where, x and y are the coordinates along and normal to the

surface, respectively. ν is the kinematic viscosity, time is denoted by *t, u* and *v* are the velocity components along the *x* and *y* directions, respectively. *K* is the permeability of the porous medium and Γ is the empirical constant in the second-order resistance. *T* is the temperature, ϕ is the solid volume fraction, $\alpha = k/(\rho C)_f$ is the thermal diffusivity, D_B is the Brownian diffusion coefficient, D_T is the thermophoretic diffusion coefficient, $\tau = (\rho C)_p/(\rho C)_f$ is the ratio of the effective heat capacity of the nanoparticle material to the heat capacity of the fluid, *g* is the acceleration due to gravity.

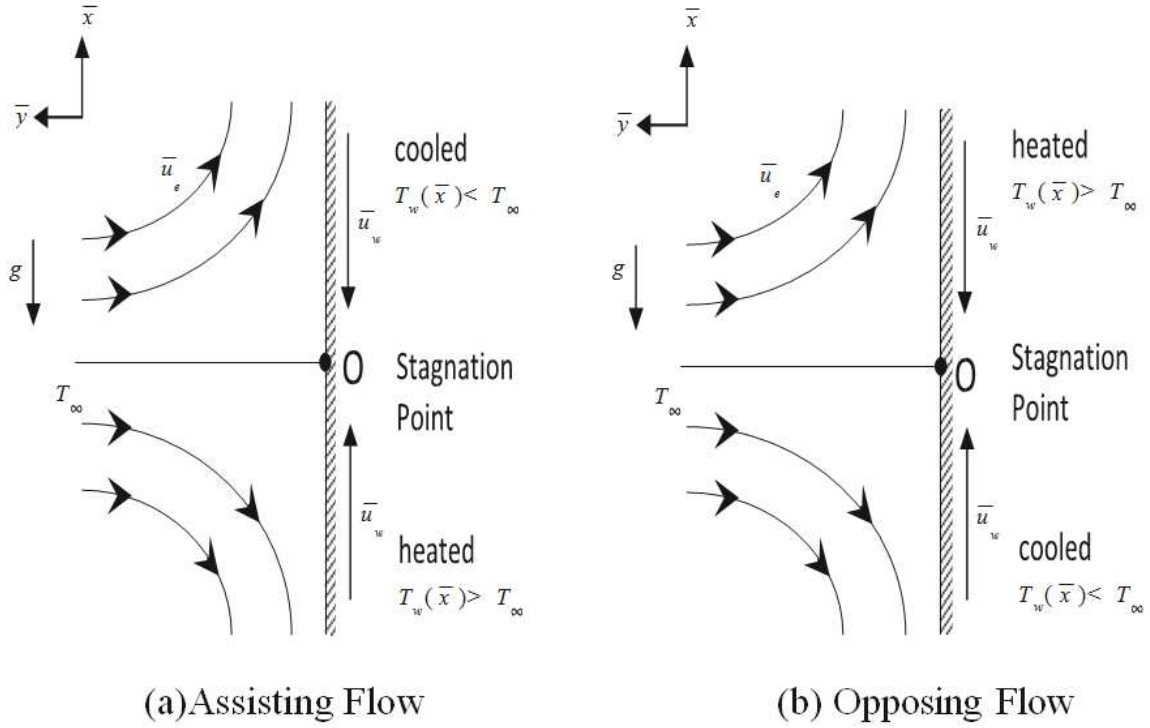

Fig. 1. *Physical model and coordinate system.*

The proposed initial conditions are

$$u(x,y,t) = v(x,y,t) = 0, \quad T(x,y,t) = T_\infty, \quad \phi(x,y,t) = \phi_\infty \text{ for } t < 0. \tag{5}$$

The proposed boundary conditions for $t \geq 0$ are

$$\begin{aligned} &u(t,x,0) = v(t,x,0) = 0, \quad u(t,x,\infty) = U_e = ax/(1-ct), \quad a > 0, \\ &T(t,x,0) = T_w(t,x) = T_\infty + bx/(1-ct)^2, \quad T(t,x,\infty) = T_\infty, \\ &\phi(t,x,0) = \phi_w(t,x) = \phi_\infty + bx/(1-ct)^2, \quad \phi(t,x,\infty) = \phi_\infty, \quad b,c > 0, \end{aligned} \tag{6}$$

where a and c are constants (with a > 0 and c ≥ 0, where ct < 1), and both have dimension time^{-1}, while b is a constant and has dimension temperature/length, with b > 0 and b < 0 corresponding to the assisting and opposing flows, respectively, and b = 0 is for forced convection limit (absence of buoyancy force).

To transform equations (1-4) into a set of ordinary differential equations, we now introduce the following dimensionless quantities; the mathematical analysis of the problem is simplified by introducing the following similarity transforms:

$$\begin{aligned} &\eta = \sqrt{\frac{a}{\upsilon(1-ct)}}\, y, \quad \psi = \sqrt{\frac{a\upsilon}{1-ct}}\, x f(\eta), \\ &\theta(\eta) = \frac{T - T_\infty}{T_w - T_\infty}, \quad \varphi(\eta) = \frac{\phi - \phi_\infty}{\phi_w - \phi_\infty} \end{aligned} \tag{7}$$

The equation of continuity is satisfied if we choose a stream function $\psi(x,y)$ such that $u = \frac{\partial \psi}{\partial y}$, $v = -\frac{\partial \psi}{\partial x}$.

Using the similarity transformation quantities (7), the governing Eqs. (2–6) are transformed to the ordinary differential equation as follows:

$$\begin{aligned} &f''' + 1 + A\left(1 - f' + \frac{1}{2}\eta f''\right) - f'^2 + f f'' + \lambda(\theta - N_r \varphi) \\ &+ \gamma(1 - f') + \Delta(1 - f'^2) = 0 \end{aligned} \tag{8}$$

$$\frac{1}{\mathrm{Pr}}\theta'' - A\left(2\theta + \frac{1}{2}\eta\theta'\right) - f'\theta + f\theta' + N_b \theta'\varphi' + N_t \theta'^2 = 0 \tag{9}$$

$$\frac{1}{Le}\varphi'' - A\left(2\varphi + \frac{1}{2}\eta\varphi'\right) - f'\varphi + f\varphi' + \frac{1}{Le}\frac{N_t}{N_b}\theta'' = 0 \tag{10}$$

With the boundary conditions:

$$\begin{aligned} &\mathrm{f}'(\eta)=0,\quad \mathrm{f}(\eta)=0,\ \theta(\eta)=0,\ \ \varphi(\eta)=0,\\ &for\ \ t<0, \end{aligned} \tag{11}$$

and proposed boundary conditions for $t \geq 0$ are

$$\begin{aligned} &\mathrm{f}(0)=0,\quad \mathrm{f}'(0)=0,\ \theta(0)=1,\ \ \varphi(0)=1,\\ &\mathrm{f}'(\infty)=1,\ \theta(\infty)=0,\ \ \varphi(\infty)=0, \end{aligned} \tag{12}$$

Where the governing parameters are defined as:

$$\begin{aligned} &A=\frac{c}{a},\ \ \mathrm{Pr}=\frac{\nu}{\alpha},\ \ Le=\frac{\nu}{D_B},\ \ \lambda=\frac{Gr_x}{\mathrm{Re}_x^2},\\ &\gamma=\frac{1}{Da_x\,\mathrm{Re}_x},\ \Delta==\frac{\Gamma}{Da_x^{1/2}}N_b=\frac{\tau}{\nu}D_B\left(\phi_w-\phi_\infty\right),\\ &N_t=\frac{\tau}{\nu}\left(\frac{D_T}{T_\infty}\right)\left(T_w-T_\infty\right),\ N_r=\frac{(\rho_p-\rho_f)(\phi_w-\phi_\infty)}{\rho_f\beta_T(1-\phi_\infty)(T_w-T_\infty)} \end{aligned} \tag{13}$$

Where f', θ and φ are the dimensionless velocity, temperature and particle concentration, respectively. The prime denotes differentiation with respect to the similarity variable η . $Gr_x=\frac{g\beta(T_w-T_\infty)x^3}{\nu^2}$, $\mathrm{Re}_x=\frac{U_e x}{\nu}$ and $Da_x=\frac{K}{x^2}$ are Grashof, Reynolds and Darcy numbers, respectively. *A, λ, Pr, Le, N_T, N_B, N_r, γ* and *Δ* denotes the unsteadiness parameter, mixed convection parameter, Prandtl number, Lewis number, thermophoresis parameter, Brownian motion parameter, nanofluid buoyancy ratio, first resistant parameter and second resistant parameter, respectively.

The important physical quantities of interest in this problem are the skin friction coefficient (wall shear stress) C_f, local Nusselt number Nu_x and the local Sherwood number Sh_x that are defined as:

$$\begin{aligned} &C_f=\frac{\mu}{\rho U_\infty^2}\left(\frac{\partial u}{\partial y}\right)_{y=0},\quad Nu_x=\frac{x}{(T_w-T_\infty)}\left(\frac{\partial \theta}{\partial y}\right)_{y=0},\\ &Sh_x=\frac{x}{(\phi_w-\phi_\infty)}\left(\frac{\partial \phi}{\partial y}\right)_{y=0} \end{aligned} \tag{14}$$

Substituting Eq. (7) into Eq. (18), we get

$$\begin{aligned} &C_f=\mathrm{Re}_x^{-1/2}\,f''(0),\ \ Nu_x=-\mathrm{Re}_x^{-1/2}\,\theta'(0),\\ &Sh_x=-\mathrm{Re}_x^{-1/2}\,\varphi'(0) \end{aligned} \tag{15}$$

3. Results and Discussion

The resulting differential systems (8)–(10) subjected to the boundary conditions (12) are solved numerically through fourth-fifth order Runge–Kutta method (RK45) using a shooting technique. The values of the governing parameters are chosen arbitrary. However, the numerical results are presented for some representative values of these governing parameters. In order to see the physical insight, the numerical values of velocity $f'(\eta)$, temperature $\theta(\eta)$, and nanoparticle volume fraction $\varphi(\eta)$ with the boundary layer have been computed for different parameters as unsteadiness parameter A , mixed convection parameter λ ,nanofluid buoyancy ratio parameter N_r , thermophoresis parameter N_t , Brownian motion parameter N_b , first resistant parameter γ , second resistant parameter Δ . Prandtl number Pr and Lewis number Le .

Table 1 indicates results for wall values for the gradients of velocity, temperature and volume fraction functions which are proportional to the friction factor, Nusselt number and Sherwood number, respectively. From this table, we notice that as N_r increases, the friction factor increases, the heat transfer rate (Nusselt number) and mass transfer rate (Sherwood number) decrease. As N_t and N_b increase, the friction factor and surface mass transfer rates increase whereas the surface heat transfer rate decreases

Table (1). *Effect of Nt, Nb and Nr on f``(0), θ`(0) and ϕ`(0)with A=0.5, λ=1, γ=0.5, Δ =0.5, Pr=10 and Le=10*

N_b	N_t	N_r=0.5			N_r=1			N_r=3		
		f``(0)	-θ`(0)	-ϕ`(0)	f``(0)	-θ`(0)	-ϕ`(0)	f``(0)	-θ`(0)	-ϕ`(0)
	0.1	1.86358	1.98266	2.99959	1.75281	1.97640	2.97942	1.29405	1.94971	2.89209
	0.3	1.87689	1.46341	3.00885	1.74724	1.46030	2.96609	1.20280	1.44720	2.77490
0.1	0.5	1.89459	1.18916	3.30288	1.75777	1.18808	3.23693	1.17626	1.18396	2.93645
	0.7	1.91206	1.02290	3.60614	1.77309	1.02289	3.52129	1.17597	1.02359	3.12943
	0.9	1.92805	0.91043	3.88186	1.78917	0.91098	3.78222	1.18647	0.91421	3.31690
	0.1	1.91563	1.10471	3.50357	1.82008	1.10377	3.48831	1.42727	1.09997	3.42351
	0.3	1.93714	0.89987	3.66024	1.83864	0.89972	3.64082	1.43308	0.89932	3.55799
0.3	0.5	1.95564	0.78110	3.80811	1.85644	0.78133	3.78544	1.44766	0.78250	3.68860
	0.7	1.97137	0.70268	3.93471	1.87243	0.70308	3.90958	1.46449	0.70499	3.80212
	0.9	1.98482	0.64593	4.04428	1.88657	0.64642	4.01722	1.48123	0.64867	3.90151
	0.1	1.94644	0.69021	3.53118	1.85358	0.69053	3.51722	1.47246	0.69207	3.45816
	0.3	1.96535	0.60599	3.66488	1.87203	0.60649	3.64911	1.48897	0.60871	3.58235
0.5	0.5	1.98126	0.55157	3.77327	1.88824	0.55213	3.75618	1.50642	0.55460	3.68382
	0.7	1.99473	0.51253	3.86302	1.90230	0.51310	3.84492	1.52299	0.51563	3.76836
	0.9	2.00627	0.48247	3.93986	1.91454	0.48304	3.92098	1.53822	0.48556	3.84111

	0.1	1.96866	0.48162	3.52373	1.87681	0.48224	3.51037	1.50008	0.48497	3.45396
	0.3	1.98501	0.44299	3.63003	1.89347	0.44363	3.61569	1.51811	0.44640	3.55514
0.7	0.5	1.99883	0.41555	3.71507	1.90787	0.41617	3.70001	1.53507	0.41889	3.63650
	0.7	2.01059	0.39448	3.78574	1.92032	0.39508	3.77015	1.55044	0.39771	3.70439
	0.9	2.02073	0.37744	3.84655	1.93115	0.37802	3.83051	1.56425	0.38055	3.76297

The effects of the first and second resistances of the porous medium on the gradients of velocity, temperature and volume fraction functions are been illustrated in Table 2. From this table we conclude that both the first and second resistances enhance the wall shear stress and the mass transfer rate and reduce the heat transfer rate.

Table (2). *Effects of γ and Δ on f`(0) , $-\theta$` (0) and -ϕ` (0) with A=0.5, λ=1, N_T=0.5, N_B=0.5, N_R=1, Pr=10 and Le=10*

γ	Δ	f`(0)	-θ(0)	-ϕ(0)
0.0	0. 0	1.74114	0.55465	3.71225
	2.0	2.42814	0.54777	3.86815
	4.0	2.94365	0.54481	3.96362
	6.0	3.37615	0.54328	4.03332
2.0	0. 0	2.27894	0.54976	3.82839
	2.0	2.82588	0.54591	3.93648
	4.0	3.27555	0.54397	4.01254
	6.0	3.66738	0.54292	4.07146
4.0	0. 0	2.69411	0.54729	3.90496
	2.0	3.16479	0.54480	3.98909
	4.0	3.56984	0.54347	4.05272
	6.0	3.93132	0.54275	4.10394
6.0	0. 0	3.05265	0.54579	3.96396
	2.0	3.47213	0.54411	4.03302
	4.0	3.84350	0.54318	4.08770
	6.0	4.18059	0.54269	4.13297

We computed the solutions for the dimensionless velocity, temperature and nanoparticle volume fraction in Figs. 2–10. The effects of all the parameters governing the problem are discussed.

The variation of the non-dimensional velocity, temperature and nanoparticle concentration for $N_t = 0.5, N_b = 0.5, N_r = 1.0, \lambda = 1.0, \Pr = 10, Le = 10, \gamma = 0.5, \Delta = 0.5$ with unsteadiness parameter A is illustrated in Fig. 2. It can be observed from Fig. 2(a) that first for velocity distribution, there is a special point ($\eta \approx 1.4$) called 'crossing over point' and the velocity profiles have completely conflicting behavior before and after that point. The value of the velocity profile for fixed η increases before that point and slightly decreases after that. Thus, due to the increase of unsteadiness parameter, A, the velocity initially enhances but ultimately it increases the thickness of momentum boundary layer. On the other hand the temperature and nanoparticle volume fraction profiles of Figs. 2 (b, c), show that the unsteadiness controls the heat and mass transfer. The control of heat and mass transfer is of great practical significance. For the increase of A, the temperature and nanoparticle volume fraction at a point decreases because the thermal boundary-layer thickness rapidly decreases due to increase of unsteadiness.

The effect of mixed convection parameter λ on the non-dimensional velocity, temperature and nanoparticle volume fraction is illustrated in Fig. 3. From these figures, it is observed that the velocity is increased as λ increase, but both the temperature and nanoparticle fraction decrease with increasing λ.

The velocity profile decreases and both the temperature and nanoparticle volume fraction increases as nanofluid buoyancy ratio parameter N_r increases as showed in in Fig. 4.

Figure5 presents the effect of thermophoresis N_t on the velocity, temperature and volume fraction distributions. It is observed that the momentum boundary-layer thickness increases with an increase of N_t . As the parameter N_t increases, the thermal and nanoparticle volume fraction boundary-layer thickness increase for the specified conditions.

Furthermore, increasing the value of the Brownian motion N_b causes a thickening of momentum and thermal boundary layers, whereas thinning of the nanoparticle volume fraction boundary layer as shown in Fig.6. Physically, it is true due to the fact that the large values of the Brownian motion parameter impacts a large extent of the fluid. It results in the thickening of the momentum and thermal boundary layers. Hence, the present analysis shows that the flow field is appreciably influenced by the Brownian motion N_b.

The effect of both first resistant parameter γ and second resistant parameter Δ is showed in Fig. 7 and Fig. 8, respectively. From these figures, it is observed that both γ and Δ have the same behavior. The velocity profile increases but the temperature profile and volume fraction profile decreases as both γ and Δ increases.

The effect of Prandtl number Pr is illustrated in Fig. 9. From these figures, it is observed that as Pr increases the velocity and temperature profiles decrease. On the other hand, for the volume fraction profiles there is a crossing over point at ($\eta \approx 0.5$) where the volume fraction profile decreases before that point and slightly increases after that.

It is noticed, from Fig. 10 that an increase in the Lewis number *Le* results in an increase in the velocity, but in a decrease of the volume fraction within the boundary layer. In the temperature profile there is a crossing over point at ($\eta \approx 0.8$) where the temperature profiles have completely conflicting behavior before and after that point. The value of the temperature profile for fixed η decreases before that point and slightly increases after it. The present analysis shows that the flow field is appreciably influenced by the Lewis number *Le*.

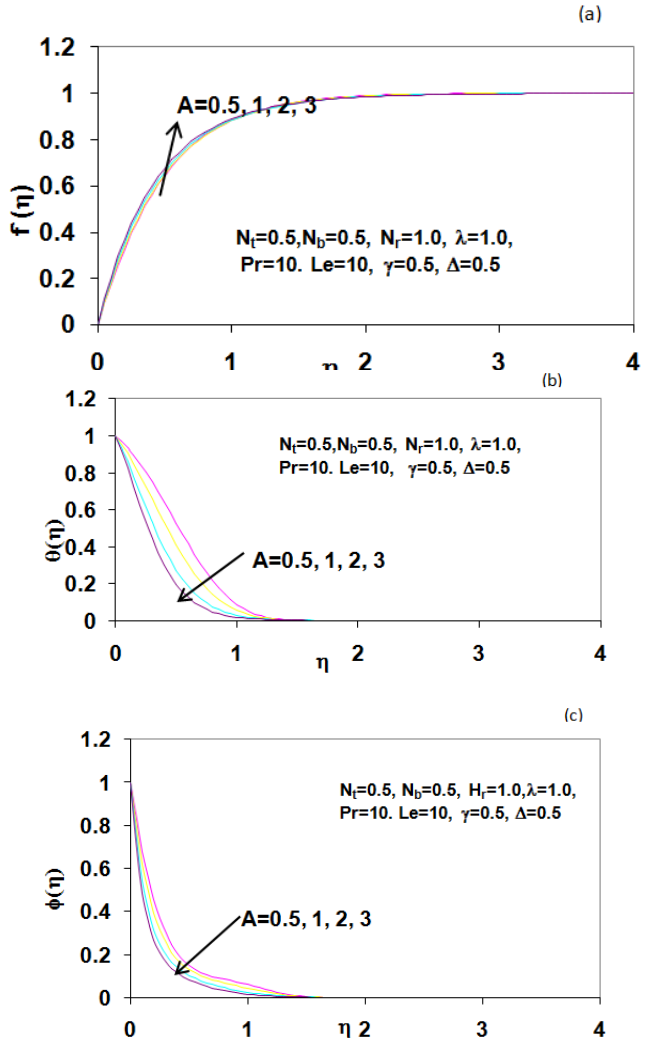

Fig. 2. *Effects of unsteadiness parameter A on (a) velocity, (b) Temperature and (c) Nanoparticle volume fraction profiles.*

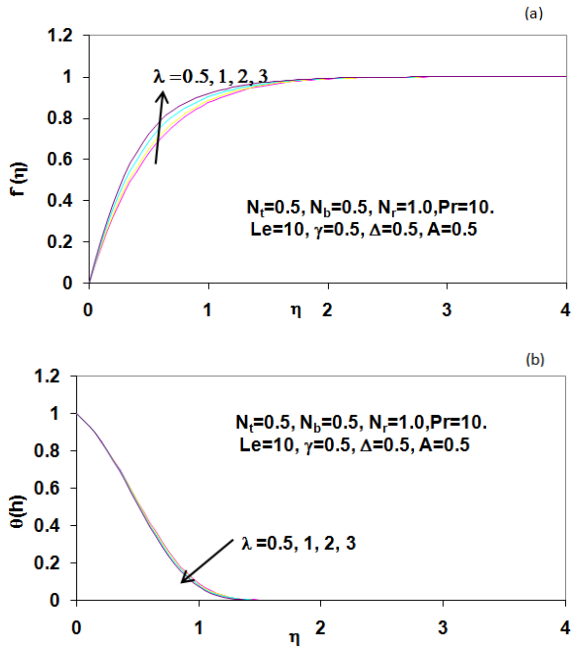

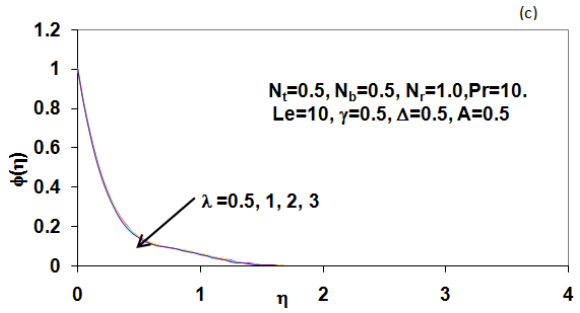

Fig. 3. *Effects of mixed convection parameter λ on (a) velocity, (b) Temperature and (c) Nanoparticle volume fraction profiles.*

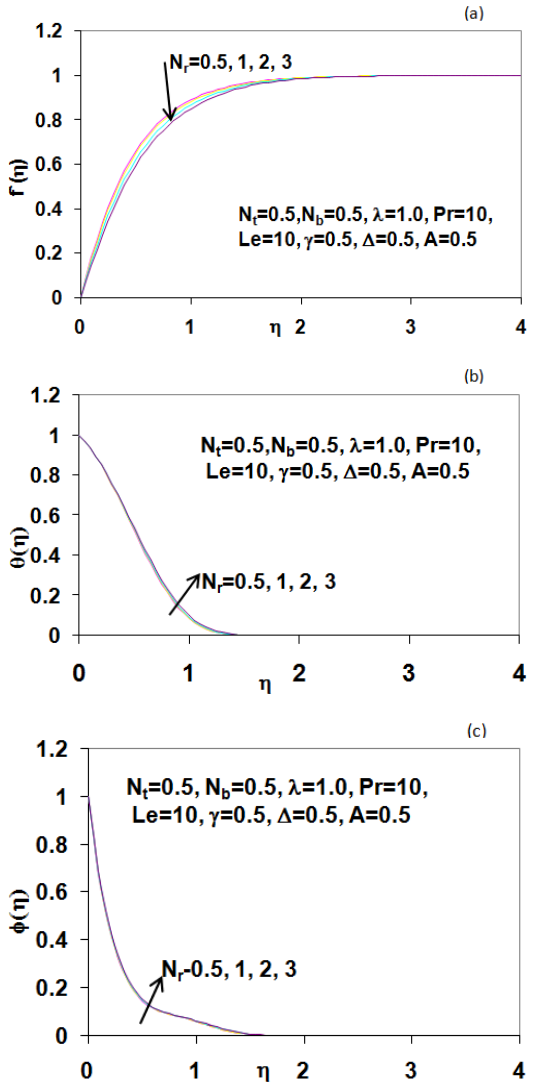

Fig. 4 *Effects of nanofluid buoyancy ratio parameter N_r on (a) velocity, (b) Temperature and (c) Nanoparticle volume fraction profiles.*

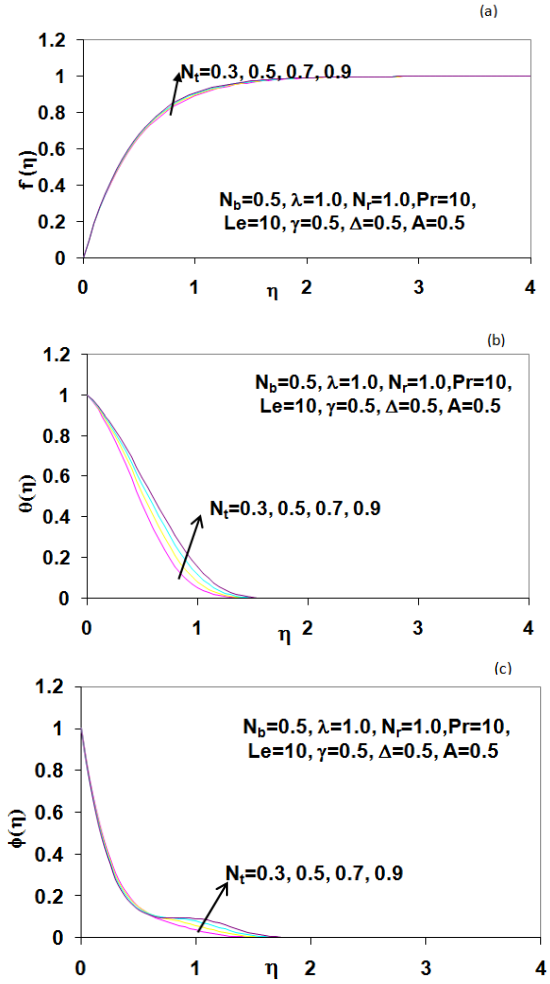

Fig. 5. *Effects of thermophoresis parameter* N_t *on (a) velocity, (b) Temperature and (c) Nanoparticle volume fraction profiles.*

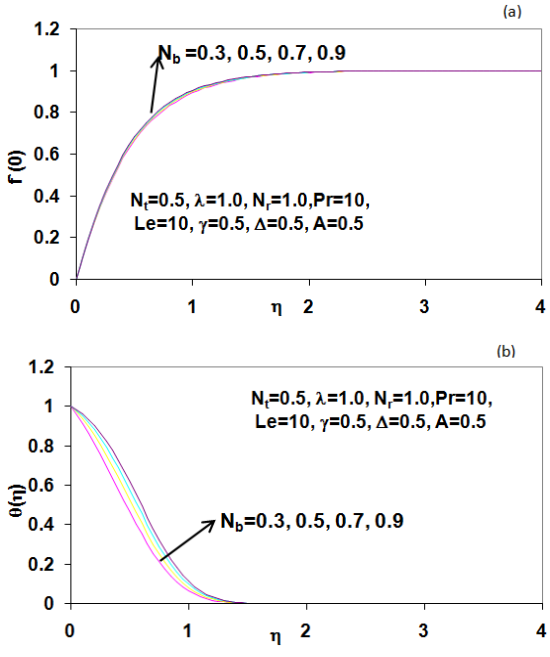

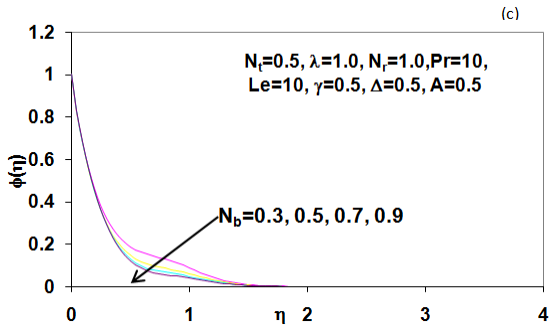

Fig. 6. *Effects of Brownian motion parameter* N_b *on (a) velocity, (b) Temperature and (c) Nanoparticle volume fraction profiles.*

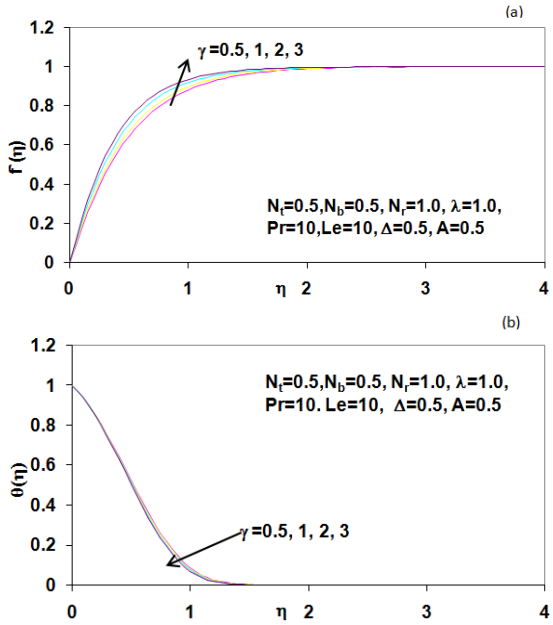

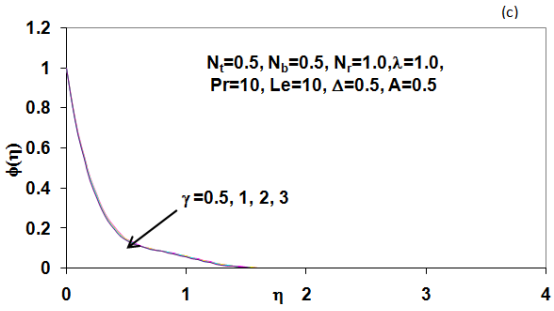

Fig. 7. *Effects of first resistant parameter* γ *on (a) velocity, (b) Temperature and (c) Nanoparticle volume fraction profiles.*

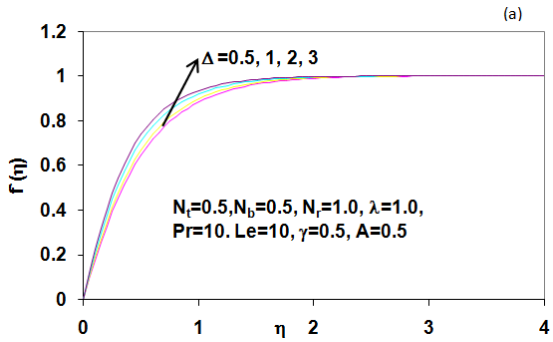

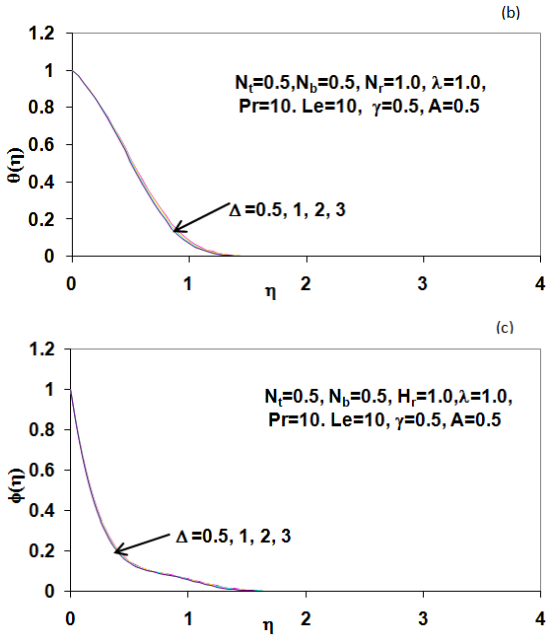

Fig. 8. Effects of second resistant parameter Δ *on (a) velocity, (b) Temperature and (c) Nanoparticle volume fraction profiles.*

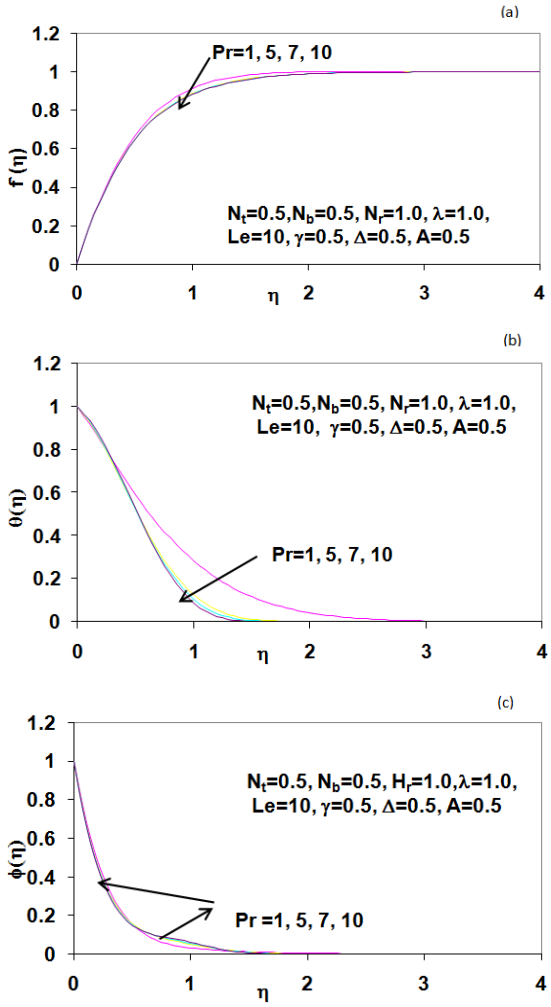

Fig. 9. Effects of Prandtl number Pr *on (a) velocity, (b) Temperature and (c) Nanoparticle volume fraction profiles.*

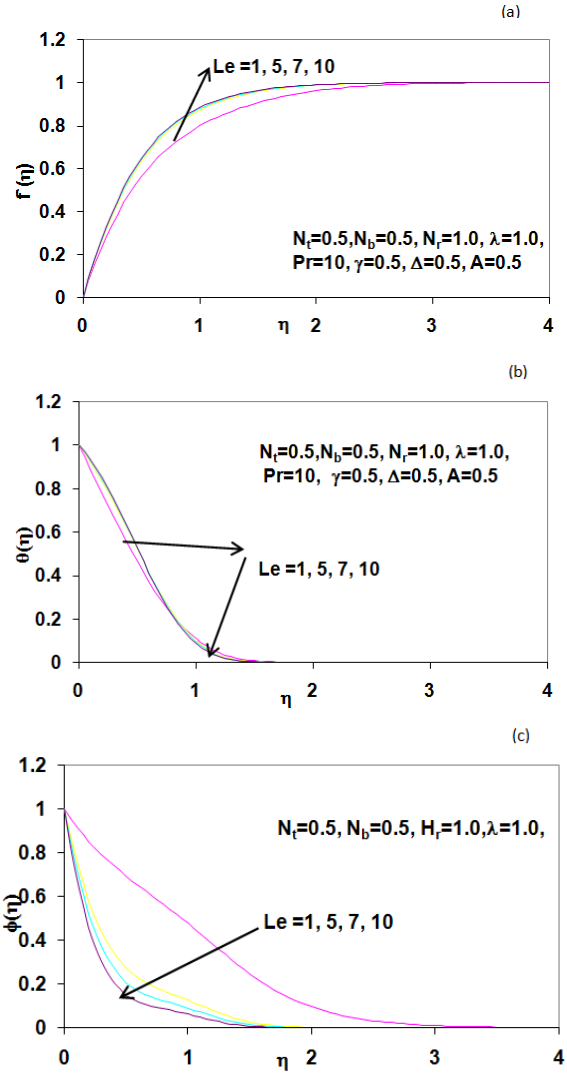

Fig. 10. Effects of Lewis number Le *on (a) velocity, (b) Temperature and (c) Nanoparticle volume fraction profiles.*

4. Conclusions

In the present work, we studied theoretically the problem of unsteady mixed convection boundary-layer flow near a stagnation point of a heated vertical surface embedded in a nanofluid-saturated porous medium. The resulting system of nonlinear partial differential equations is transformed to a system of ordinary differential equations by the means of self-similar solution. The obtained system is solved numerically using an efficient numerical shooting technique with a fourth-fifth order Runge–Kutta method scheme (MATLAB package). The solutions for the flow, heat and mass transfer characteristics are evaluated numerically for various values of the governing parameters, namely unsteadiness parameter A, mixed convection parameter λ, nanofluid buoyancy ratio parameter N_r, thermophoresis parameter N_t, Brownian motion parameter N_b, first resistant parameter γ, second resistant parameter Δ. Prandtl number Pr and Lewis number Le.

The following are brief summary conclusions drawn from

the analysis:

1. The magnitude of the skin friction coefficient $f''(0)$ increases, while the local Nusselt number decreases with increasing the nanofluid parameters N_t, N_b and N_r.

2. The local Sherwood number increases as both N_t and N_b parameter increases. However, it decreases as N_r increases.

3. The thickness of momentum boundary layer decreases with an increase in nanofluid buoyancy ratio parameter N_r and Prandtl number Pr . However, it increases with increasing all other parameters.

4. The thickness of thermal boundary layer increases with an increase in the nanofluid parameters N_t, N_b and N_r.

5. The nanoparticle volume fraction boundary-layer thickness increases with an increase in both N_t and N_r parameters and decreases with an increase in N_b parameter.

6. Both the first and second resistance parameters γ and Δ enhanced the momentum boundary-layer thickness and reduced both the thermal and nanoparticle volume fraction boundary-layer thickness

Acknowledgement

The authors would like to thank National Science, Technology and Innovation Plan (NSTIP) at Kingdom of Saudi Arabia (Project ID 12-MAT2296-10) for the financial support.

Nomenclature

A	Unsteadiness parameter
a,b,c	Constants in Eq. (6)
C_f	Skin friction coefficient
D_a	Darcy number
D_B	Brownian diffusion coefficient
D_T	Thermophoresis diffusion coefficient
f	dimensionless stream function
G	Acceleration due to gravity
Gr	Grashof number
Le	Lewis number
k	Thermal conductivity
K	Permeability
N_b	Brownian motion parameter
N_r	Nanofluid buoyancy ratio parameter
N_t	Thermophoresis parameter
Pr	Prandtl number
Re	Local Reynolds number
Sh	Sherwood number
t	Time
T	Fluid temperature
T_w	Temperature at the surface
T_∞	Ambient temperature as y tends to infinity
u,v	Velocity components along x and y directions, respectively
x,y	Distances along and normal to the surface

Greek symbols

α	Thermal diffusivity
β	Coefficient of volumetric thermal expansion
φ	Dimensionless nanoparticle volume fraction
Γ	Empirical constant
η	Pseudo similarity variable
θ	Dimensionless temperature
λ	Buoyancy parameter
μ	Coefficient of viscosity
γ	First order resistance
$\frac{\partial u}{\partial x}+\frac{\partial v}{\partial y}=0$	Second order resistance
ν	Kinematic viscosity

Subscripts

e,w,∞	Conditions at the edge of the boundary layer, at the surface and in the free stream

References

[1] Ramachandra N., Chen T. and Armaly B, 1988. Mixed convection in the stagnation flows adjacent to vertical surface, J. Heat Transfer Vol. 110, pp. 173-177.

[2] Scshadri R., Srccshylan N. and Nath G., 2002. Unsteady mixed convection flow in the stagnation region of a heated vertical plate due to impulsive motion, Int. J. Heat and Mass Transfer Vol. 45 pp. 1345-1352.

[3] Hall M., 1969. The boundary layer over an impulsively started flat plate, Proc. R. Soc. Vol. 310A, pp. 401-414.

[4] Dennis S., 1972. The motion of a viscous fluid past an impulsively started semi-infinite flat plate, J. Inst. Math. It's Appl. Vol. 10, pp. 105-117.

[5] Watkins C., 1975. Heat transfer in the boundary layer over an impulsively started flat plate, J. Heat Transfer Vol. 97, pp. 492-484.

[6] Smith S., 1967. The impulsive motion of a wedge in a viscous fluid, Z. Angew. Math. Phys. Vol. 18 , pp. 508-522.

[7] Nanbu K., 1971. Unsteady Falkner Skan flow, Z. Angew. Math. Phys. Vol. 22, pp. 1167-1172.

[8] Williams J. and Rhyne T.,1980. Boundary layer development on a wedge impulsively set into motion, SIAM J. Appl. Math. Vol. 38, pp. 215-224.

[9] Kumari M., 1997. Development of flow and heat transfer on a wedge with a magnetic field, Arch. Mech. Vol. 49, pp. 977-990.

[10] Ece M., 1992. An initial boundary layer flow past a translating and spinning rotational symmetric body, J. Eng. Math. Vol. 26, pp. 415-428.

[11] Ozturk A. and Ece M., 1995. Unsteady forced convection heat transfer from a translating and spinning body, J. Energy Rcsour. Tcchnol. Vol. 117, pp. 318-323.

[12] Brown S. and Riley N., 1973. Flow past a suddenly heated vertical plate, J. Fluid Mech. Vol. 59, pp. 225-237.

[13] Ingham D., 1985. Flow past a suddenly heated vertical plate, Proc. R. soc. Vol. 402A, pp. 109-134.

[14] Amin N. and Riley N., 1995. Mixed convection at a stagnation point, Quart. J. Mech. Vol. 48, pp. 111-121.

[15] Hassanien I., Ibrahim, F. and Omer Gh.,2004. Unsteady free convection flow in the stagnation-point region of a rotating sphere embedded in a porous medium, Mech.Mech. Eng. Vol. 7, pp. 89-98.

[16] Hassanien, I., Ibrahim, F. and Omer Gh.,2006. Unsteady flow and heat transfer of a viscous fluid in the stagnation region of a three-dimensional body embedded in a porous medium, J.Porous Media, Vol. 9, pp. 357-372.

[17] Hassanien, I. and Al-Arabi, T.,2008. Thermal Radiation and variable viscosity effects on unsteady mixed convection flow in the stagnation region on a vertical surface embedded in a porous medium with surface heat flux Vol. 29, pp. 187 – 207.

[18] Yacob N., Ishak A. and Pop I., 2011. Falkner–Skan problem for a static or moving wedge in nanofluids. Int J Thermal Sci. Vol 50, pp. 133–139.

[19] Congedo P., Collura S. and Congedo P., 2009.Modeling and analysis of natural convection heat transfer in nanofluids. In: Proc ASME Summer Heat TransferConf. Vol. 3,pp. 569–579.

[20] Hamad M., Pop I. and Ismail A. 2011. Magnetic field effects on free convection flow of a nanofluid past a semi-infinite vertical flat plate. Nonlinear Analysis:Real World Appl. Vol. 12, pp. 1338–1346.

[21] Buongiorno J., 2006. Convective transport in nanofluids. ASME J Heat Transfer.Vol. 128, pp. 240–250.

[22] Hamad M., 2011. Analytical solution of natural convection flow of a nanofluid over a linearly stretching sheet in the presence of magnetic field. Int. Commun. Heat Mass Transfer. Vol. 38, pp. 487–492.

[23] Khan W and Pop I.,2010. Boundary-layer flow of a nanofluid past a stretching sheet. Int. J Heat Mass Transfer. Vol. 53, pp. 2477–2483.

[24] Abu-Nada E. and Chamkha A., 2010. Effect of nanofluid variable properties on natural convection in enclosures filled with a CuO–EG–water nanofluid. Int. J. Thermal Sci. Vol. 49, pp. 2339–2352.

[25] Das S., S Choi SU, Yu W. and Pradeep T., 2007. Nanofluids: Science and Technology. New Jersey: Wiley.

[26] Kakaç S. and Pramuanjaroenkij A., 2009. Review of convective heat transfer enhancement with nanofluids. Int. J Heat Mass Transfer. Vol. 52, pp. 3187–3196.

[27] Muthtamilselvan M., Kandaswamy P. and Lee J., 2010. Heat transfer enhancement of copper–water nanofluids in a lid-driven enclosure. Commun Nonlinear Sci. Numer. Simulat. Vol. 15, pp. 1501–1510.

[28] Pereyra V.,1978. PASVA3, an adaptive finite difference FORTRAN program for first order non-linear boundary value problems, in: Lecture Note in Computer Science, Vol. 76, Springer, Berlin.

[29] Scshadri R., Srccshylan N. and Nath G., 2002. Unsteady mixed convection flow in the stagnation region of a heated vertical plate due to impulsive motion, Int. J. Heat and Mass Transfer Vol. 45 pp. 1345-1352.